Title:

A minimal "push-pull" bistability model explains oscillations between quiescent and proliferative cell states.

Sandeep Krishna[a,1] and Sunil Laxman[b,1]

[a]Simons Centre for the study of Living Machines, National Centre for Biological Sciences.
[b]Institute for Stem Cell Biology and Regenerative Medicine.
GKVK post, Bellary Road
Bangalore 560065

[1]Correspondence: sandeep@ncbs.res.in, sunil@instem.res.in

Abstract

A minimal model for oscillating between quiescent and growth states, dependent on the availability of a metabolic resource, is presented. From the yeast metabolic cycles (YMCs), metabolic oscillations in oxygen consumption are represented as transitions between quiescent and growth states. We consider metabolic resource availability, growth rates, and switching rates (between states) to model a relaxation oscillator explaining transitions between these states. This bistability model reveals a required communication between the metabolic resource that determines oscillations, and the quiescent and growth state cells. Cells in each state reflect memory, or hysteresis of their current state, and "push-pull" cells into the other state. Finally, a parsimonious argument is made for a specific central metabolite as the controller of switching between quiescence and growth states. We discuss how an oscillator built around the availability of such a central metabolic resource is sufficient to regulate oscillations between growth and quiescence, through committed transitions.

Keywords: quiescence, growth, metabolic cycles, bistability, acetyl-CoA, NADPH

Introduction

While all cells can exist in a variety of states, two opposite ends of the spectrum are the "growth" state (leading to mitotic division and proliferation), or a non-proliferative "quiescent" state. The quiescent state, operationally defined here as a reversibly non-dividing state, is the predominant state of all living cells (1, 2). Understanding how cells reversibly transition from a

quiescent to a growth state is therefore a fundamental biological question. Current explanations for how cells commit to growth and cell division account for metabolic regulation, biomolecule synthesis, and regulated progression through the cell cycle, presenting multiple, integrated mechanisms of information transfer within a cell that lead to the eventual growth outcome.

However, when a population of genetically identical cells are present in a uniform environment, how can individual cells within such a population decide to switch between a quiescent (effective "G_0") state and a growth/proliferation state? Indeed, such heterogeneity of cell states within populations is widely observed and acknowledged. Numerous examples exist in nearly all systems studied, from simple eukaryotes like the budding yeast, to complex mammalian systems (3–9), with multiple molecular events correlating with transitions between growth and quiescence. For any population transitioning into either of these states, experimentalists have asked: (i) what hallmarks allow discrimination between actively proliferating and G_0 cells? (ii) how do cells transit back and forth between these two states? And (iii) how are different signals processed and integrated into an appropriate cellular response? The regulation of the final cellular outcome occurs at multiple levels, including differential gene expression programs, and signaling responses to growth factors, which can be different depending upon the type of cell or organism studied. However, at its very core, this transition between quiescent and growth states is a metabolic problem; cells must be in a metabolic state capable of committing to growth/proliferation and must sense this state, which pushes cells towards growth. Indeed, several lines of evidence now reiterate a primary metabolic determinant for cells committing to a growth state (exiting quiescence), or remaining in a quiescent state (7–15). Given this absolute metabolic requirement to switch to growth, if there is an isogenic ("identical") population of cells present in a uniform environment, how can there be a two-state outcome where some cells undergo growth/proliferation, while the rest remain quiescent? Surprisingly, there are few rigorous theoretical, mathematical models that can provide a conceptual framework sufficient to explain this, and which will provide predictions that can be experimentally conceptualized and tested at a molecular level. This is in contrast to the extensive, elegant, and often prescient models that have been built to explain progress through the classical cell division cycle (CDC), by incorporating existing experimental data of phase-specific cell-cycle activators and inhibitors (16–19). Such modeling of the CDC has a long history (examples include (18–23)), and these types of theoretical studies have revealed biological possibilities that were experimentally determined much later (such as (24–27)).

Given this, there is considerable value in building coarse-grained but rigorous theoretical models to understand switching between quiescence and growth states. Here, the switching between quiescence and growth states could be treated as a biological oscillation (17, 19, 25, 28), while considering a dependence on a metabolic "resource" as a driver of the oscillator. For building such a model, we require extensive experimental data from biological systems where metabolic oscillations are demonstrably closely coupled with exiting quiescence/entering the CDC. Such data are readily available from the budding yeast, *S. cerevisiae*. Yeast have been the instrumental cellular model in revealing processes that define both the CDC (29) and the quiescence cycle (1, 7–9, 30). The classical CDC involves progression through the G1, S, and G2/M phases. In contrast, during a quiescence (or effective "G0") cycle, cells remain non-

dividing, but can exit quiescence and enter the G1 phase of the cell cycle to subsequently complete the CDC. Experimentally dissecting specific processes driving entry into, and exit from, quiescence (into the CDC) is challenging in asynchronous, heterogeneous cultures of cells. However, metabolically synchronized yeast populations (as manifest by oscillations in oxygen consumption) have long been studied in yeast cultures limited for a carbon source (glucose or ethanol), and subsequently fed continuously with limited concentrations of glucose or ethanol (31, 32). Gene expression studies from such glucose-limited **yeast metabolic cycles** (YMCs) showed that a majority of the genome is expressed highly periodically, further revealing the molecular organization of growth and quiescent states (12, 33–35). Genes associated with biosynthesis and growth (comprehensively described in (36)) typically peak during a high oxygen consumption phase in the YMC (33, 37–39), while genes that mark autophagy, vacuolar function and a “quiescence” state peak during a steady, low oxygen consumption phase. Strikingly, in these continuous YMC cultures, cell division is tightly gated to a temporal window. Cells divide synchronously only once during each metabolic cycle (33, 40–42) and remain in a non-dividing state during the rest of the cycle. The non-dividing population in the low oxygen consumption phase exhibits most hallmarks of quiescent cells (7, 33, 43–45). Furthermore, in each YMC, during the tight temporal window when cells divide, the culture has two visibly distinct subpopulations: dividing and nondividing (33, 41, 42). These data have suggested a close coupling between the metabolic and the cell division cycles. Importantly, the YMC itself is metabolite/nutrient regulated, and controlled by the amount of available glucose. The distinct phases of the YMC correspondingly show a separation of metabolic processes (33, 46), and several lines of evidence suggest that key metabolite amounts are critical for entering or exiting a proliferative or a non-proliferative state (34, 43, 45–47). Thus, these studies provide an extensive resource using which a theoretical, mathematical model can be built to sufficiently explain oscillations between a “quiescent” state and a “growth” state.

Here, we use existing data from the yeast metabolic cycles to build a robust model for oscillations between a quiescent and a growth state. Importantly, the model necessitates the requirement of a tripartite communication - between the metabolic resource, the quiescent cells, and the cells exiting quiescence and entering growth - in order for the cells to sustain oscillation between these two states. The model oscillations depend on an underlying bistability, which means that cells in either state exhibit hysteresis, or memory, of their states. Finally, using this model, we show how two central metabolites, thought to be critical for entry into a growth state, satisfy the required criteria for the currency that controls oscillations between these two cell states. Collectively, we provide a coarse-grained, sufficiency model to explain how cells can oscillate between a quiescent and growth state, depending upon amounts and utilization of an internal metabolic currency.

Results

Bistable states during yeast metabolic cycles

Yeast cells grown to a high cell density (in batch culture mode) in a chemostat, and when subsequently fed limited amounts of glucose medium, spontaneously undergo robust

oscillations in oxygen consumption (YMCs) (Figure 1A) and (33, 35), with the period of each oscillation ~4 hours (Figure 1A). For these oscillations to occur, the batch culture needs to first be starved for a few hours (Figure 1A), during which time all glucose is depleted, and all cells enter a non-dividing state. After this starvation, if cells are continuously provided limited medium, the oscillations in oxygen consumption spontaneously start and continue indefinitely (Figure 1A). Comprehensive gene expression analysis across these oscillations has revealed highly periodic transcript expression (33, 48), and proteins encoded by these transcripts can be "binned" into three general classes (Figure 1B, 1C). These represent "growth genes" during the high oxygen consumption phase, followed by the rapid decrease in oxygen consumption coupled with "cell division" (Figure 1B, 1C). The cells exhibiting the "growth" signature go on to enter and complete the CDC (42). Finally, the YMC enters a state of ~stable oxygen consumption where the gene expression profile revealed a "quiescent" state (Figure 1B, 1C). Mitotic cell division is tightly gated to a narrow window (Figure 1B, 1C). Interestingly, in this phase, only a fixed fraction of the cells (~35%) (and not all cells) divide during each cycle (Figure 1D). During the stable oxygen consumption phase, there are almost no budding cells (Figure 1D). It is important to note that given that this is a controlled chemostat system, the overall cell number/density is constant throughout these oscillations (33, 35), which is important for our later model. Thus, there appears to be an observable, apparent cellular bistability occurring during these oscillations in oxygen consumption. The stable, low oxygen consumption phase can therefore be envisioned as representing the non-dividing, "quiescent" state (Q), while the rapid increase in oxygen consumption followed by the reduction in oxygen consumption phase represents the "growth" state (G) (Figure 1E). Considering this, our objective was to build a mathematical model that conceptualized the oscillations in oxygen consumption as oscillations between these two (Q and G) states. For this, we first envisaged three broad scenarios that could result in such an oscillation, and could make biological sense (Figure 1F): (i) there could be the production and secretion of a resource by a sub-population of cells ("feeders"), which is taken up by other cells that will go on to divide; (ii) there could be the secretion and accumulation of a metabolite that is sensed and taken up by only some cells (but is not consumed); (iii) there is a build up of a metabolite, which is consumed by the cells at some threshold concentration (Figure 1F). Starting from these scenarios, we built simple models to test which one could create an oscillatory system between the two states.

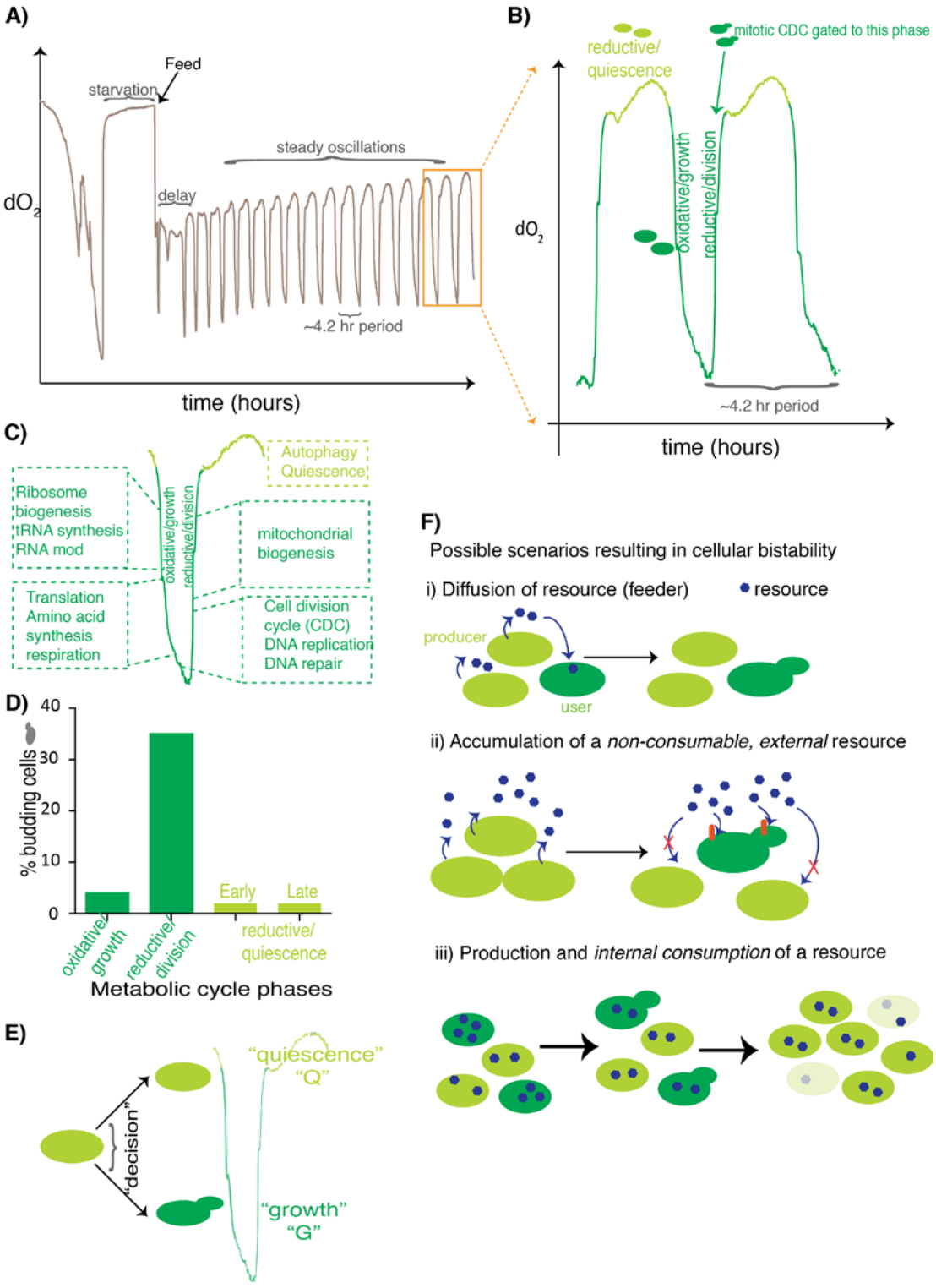

Figure 1: Apparent two-state bistability during Yeast Metabolic Cycles.

A) A representative YMC, indicating stable oscillations in oxygen consumption (based on dissolved oxygen dO_2) in yeast cultures, reflecting the yeast metabolic cycle. Note that the stable oscillations are driven by restricted feeding.

B) A more detailed illustration of each oscillation cycle, also indicating the phases of the YMC.
C) Functional outputs based on gene expression studies (from (33)), which clearly define the phases of the YMC into a general "growth/proliferation" phase, and a "quiescence" phase.
D) Observed cell division during the YMC. Cell division is tightly gated to a narrow window of the YMC. Note that only a fraction of cells, and not all cells, divide during this window of each cycle.
E) Reducing the oxygen consumption (dO_2) oscillation into a two-state (Q and G) system.
F) Plausible biological scenarios that could result in an oscillation between Q and G states.

A "push-pull" model, requiring communication between the Q state, G state and the resource, produces oscillatory behavior

Model framework for a two-state yeast population

In order to model such a two-state population of cells, the variables to consider would be the following: (a) The fraction of cells in the quiescent state (and consequently the fraction in the growth state), (b) some indicator of resource availability (dependent on the accumulation and consumption of the resource) which could modulate the switching rate between Q and G states. Thus, using this framework, we build the following equations that can describe the dynamics of a two-state population of yeast cells in a well-mixed system:

"**Change in Q population over time**": $$\frac{dq}{dt} = \nu_{GQ}(1-q) - \nu_{QG}q - \gamma q(1-q), \quad (1)$$

"**Change in resource a over time**": $$\frac{da}{dt} = \sigma - \mu\gamma(1-q)a - \gamma(1-q)a, \quad (2)$$

Here, $q \equiv Q/(G+Q)$ is the *fraction* of cells in the quiescent state, and a simply represents the concentration per cell of a `resource' (which may be intracellular or extracellular). As explained in Methods, these equations model the growth of G cells (with the growth rate being represented by the parameter γ), switching between G and Q states (ν_{GQ} and ν_{QG}), as well as the accumulation (σ) and consumption (μ) of the resource a. They also include the outflux of both cells and resource from the chemostat - because the total population of cells is known to remain approximately constant, this outflux rate necessarily depends on the growth rate of cells. By choosing which of these parameters are zero or non-zero, and how they depend on q and/or a, this framework can be used to model a variety of scenarios, which subsume the broad, biological scenarios illustrated in Figure 1E. These mathematically distinct scenarios are described below (and illustrated in Figures 2A and 2B):

1. A sub-population of feeder cells (in the Q state) secrete a resource that is sensed by other cells that can grow and divide (G state); resource accumulation σ increases with q. Such a scenario can be modelled with the G cells either consuming the resource ($\mu \neq 0$), or only sensing but not consuming the resource ($\mu = 0$) in the processes of

growing/dividing. Thus, the growth rate in the G state may be a constant, or may depend on the level of the resource (e.g., γ proportional to a). There are three sub-scenarios for how cells may switch between the two states:

   a. There is no switching between Q and G states (ν_{QG} and ν_{GQ} both zero).
   b. There is random switching between Q and G states (ν_{QG} and/or ν_{GQ} are non-zero constants).
   c. Switching between Q and G states is non-random, dependent on cell-cell communication and/or the resource level (ν_{QG} and ν_{GQ} both functions of q and/or a).

2. All cells produce and secrete a resource that is sensed only by a sub-population of (G) cells that can grow and divide, i.e., σ is a constant. As in scenario 1, the G cells may or may not consume the resource, the growth rate in the G state may or may not depend on the level of the resource, and there are three sub-scenarios for how cells may switch between the two states: no switching, random switching or non-random switching.
3. There is a build up of a resource, which is directly supplied from outside into the chemostat medium (σ is a constant). This metabolite is sensed or consumed by the G cells when they grow/divide. Again, the growth rate in the G state may or may not depend on the level of the resource and switching may work in one of three ways: none, random or non-random switching.

While scenarios (2) and (3) are mechanistically very different, they are in fact mathematically no different from each other; both result in a constant production of the resource. Hence, we need not distinguish between these two. Testing all the scenarios above, using equations 1 and 2, we find that oscillations are *not* possible in the absence of switching, or even with random switching (see Supplementary section 1), when there is no substantial time delay between resource utilization and division events (as assumed in writing equations 1 and 2). Thus, scenarios 1c, 2c and 3c are the only possibilities left. This means that the switching between Q and G states is a non-random event, and depends not only on the resource, but some form of communication between the resource, the cells in the Q state and the cells in the G state.

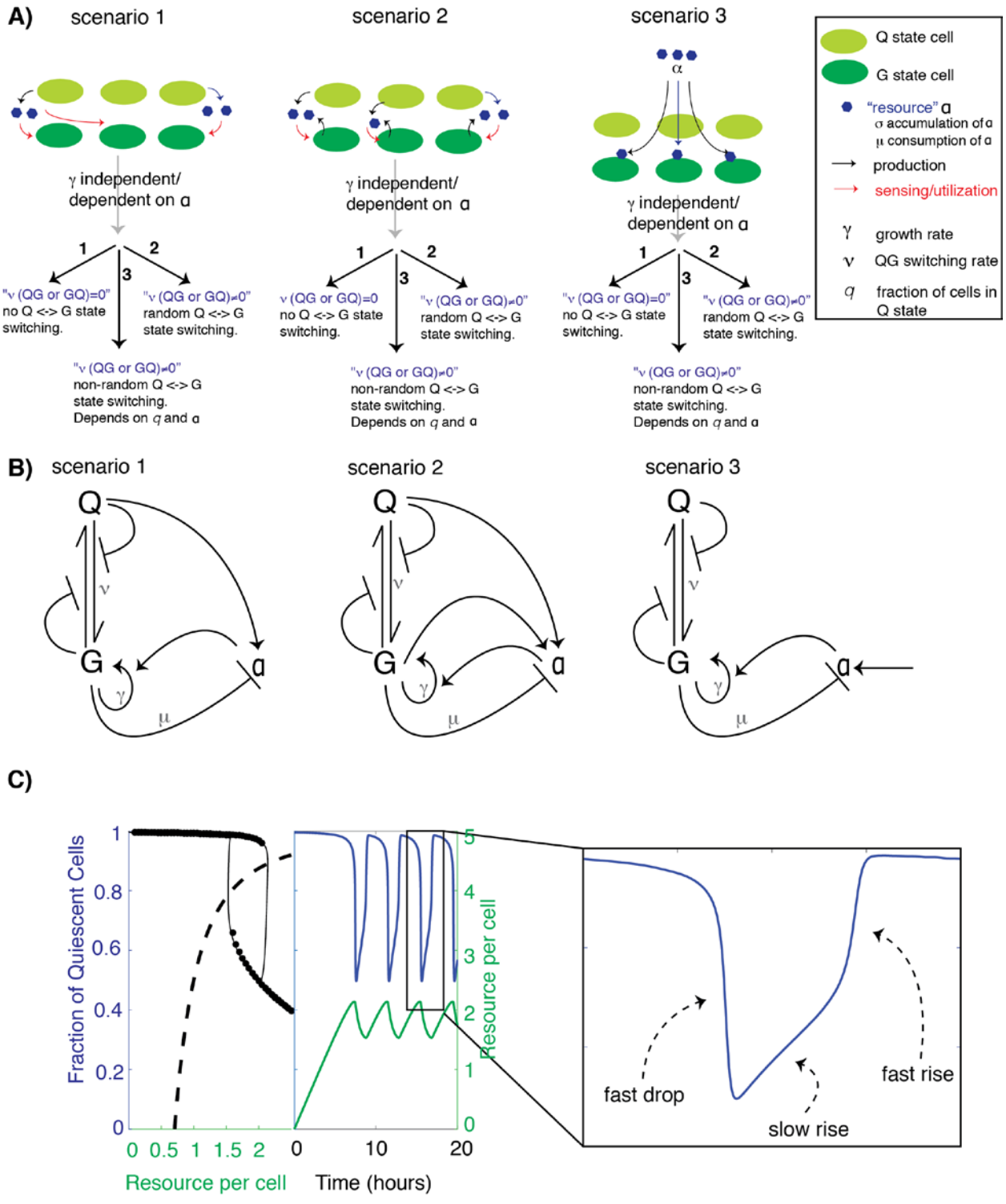

Figure 2: A "push-pull" model for bistable oscillations between Q and G states.

A) The biologically plausible scenarios from Figure 1F broken down into precise categories, and including parameters for growth rate (γ), resource (a), switching rate between Q and G states (ν), and the fraction of quiescent cells (q).

B) Schematic illustration of Figure 1A, indicating communication loops (with direction) and parameters considered, to test for possible oscillations between Q and G states.
C) A hysteretic oscillator, based on non-random switching between Q and G states, a required communication between Q, G and the resource, and a minimal cell density, and the oscillation of the amounts of resource itself that controls this Q and G oscillation (see Methods for the equations that produce this dynamics).

Hysteretic oscillator based on the two-state model

A simple way to obtain an oscillator from this two-state model uses the strategy of `frustrated bistability' previously suggested by (49). It requires two ingredients: (1) a negative feedback loop between q and a, and (2) bistability in q in the absence of the feedback. While the first can be achieved in several ways, the two simplest, biologically plausible, scenarios are where growing cells consume resource a and: (i) the growth rate γ is proportional to the resource a; or, (ii) one or both switching rates depend on a such that the net switching rate from G to Q decreases with a. Bistability in q in the absence of the feedback implies that when a is kept fixed, for some range of a values, equation 1 should allow two stable steady state levels of q, one lower and one higher. This is shown in Fig 2C left panel, where one can see the high and low `branches' traced by the solid black circles - every point on these branches is a stable steady state q can attain for the corresponding a value, using a version of equation 1 derived from scenario 3 in Fig 2B (see Methods for the full equation). When the resource a is sufficiently small, then there is only one high steady-state level possible for q. Similarly, when a is sufficiently large, there is only one low steady-state possible. However, for intermediate values of a, the system exhibits bistability and both low and high steady-state levels co-exist. In this bistable region, which steady-state level q attains depends on where it started (i.e., its 'initial condition'). Importantly, in these oscillations, the system exhibits a 'memory' (or a 'hysteresis') - the steady-state level that q eventually settles into depends on the history of the system.

When there exists such bistability, then one can get oscillations from the system described by equations 1 and 2, provided the switching rates are a few-fold faster than the rates of consumption and accumulation of the resource (49), which is a logical assumption. In that case, when q is high, a increases due to lack of consumption, so the system creeps along the high branch in Fig 2C left panel (see the trajectory traced by the thin black line) until it hits the edge of the bistable region. At that point, cells start switching to the G state, which happens relatively rapidly. Thus, the trajectory "falls off" the edge down to the low branch. On the low branch, with more G cells, the now increased consumption of the resource causes a to start decreasing, leading to the system creeping down along the low branch. When the system reaches the left edge of the bistability, the trajectory jumps up to the high branch as cells rapidly switch to the Q state. For a range of parameter values, this settles into a stable oscillation, as shown in Fig 2C middle panel, which shows how q and a vary with time as one follows the black trajectory in Fig 2C left panel.

Non-random switching is necessary for this kind of oscillation, where ν_{QG} and/or ν_{GQ} are functions of q. This can be interpreted as a form of 'quorum/cell number sensing'- implying some form of cell-cell communication (or some cell density dependent phenomenon). More

specifically, we find that choosing either ν_{QG} to be a decreasing step-function of q, or ν_{GQ} to be an increasing step-function of q (as in Fig 2C), or both, is *sufficient* to produce frustrated bistability (see supplementary Fig S1). Other shapes that we have not explored may also produce oscillations. However, our purpose here is not to find the 'best-fit' model, but rather to demonstrate the basic ingredients which are sufficient to produce hysteretic oscillations that are similar to the experimental observations. The requirement for ν_{QG} to be a decreasing step-function of q, or ν_{GQ} to be an increasing step-function of q, is basically a requirement for a "push-pull" mechanism - the more the Q cells, the more other Q cells get pulled to remain in that state, and the more G cells get pushed to switch away from their state. Irrespective of the precise molecular means by which this is achieved, cell-cell communication is a necessary ingredient for implementing such a push-pull mechanism.

Mismatch between the shape of the oscillations in the model and the experiment

The annotations in Fig 2C right panel, which zooms in to show one period of oscillation, highlight an interesting failure of the model oscillations when compared with the experimental observations. The model oscillations exhibit a fast drop in q when exiting the predominantly quiescent phase, followed by a slow(er) rise, and then a rapid rise back to a high q level. Experimentally, dO_2 levels (which we equate with q) show a fast drop, a slow *further drop*, and then a rapid rise (see Fig 1B), which is the opposite of what is seen in the present model. In the model, the shape observed arises entirely from the shape of the lower branch of q steady-states in Fig 2C, left panel. Because this lower branch starts at a q value of around 0.6-0.7 and then *decreases* as a increases, therefore there is a slow rise after the first fast drop in q. However, if such a model has to explain the shape of the experimental dO_2 oscillations, the lower branch must instead *increase* as a increases. We can show that this is not possible when the only way the resource affects the quiescent fraction is via γ being proportional to a, as in the equations that produced Fig 2C (see supplementary Fig S2). Instead, one way to produce a shape that matches experiments is by making the following choice within scenario 3c: γ (growth rate) constant, ν_{QG} a decreasing step-function of q such that the position of the step (the value of q at which the step occurs - K in Fig 3A) increases with a, and both the high and low levels of the step decrease with a (see Fig 3A, and the full equations in Methods). In that case, as shown in Fig 3B, the equations produce the correct (fast drop -> slow drop -> fast rise) shape.

What do the above choices on parameters mean in terms of processes potentially happening in the cells? A simple possible explanation for this is that even within each state (Q or G), there is a heterogeneity in the population. This can arise, for example, from differences in the amounts of an internal resource within each cell, which in turn can affect the switching rate. Our model and equations may therefore represent a broader, coarse-grained effective behavior of the switching rate, which is averaged over many cells, all of which differ a bit from each other, but are distinguished sufficiently between the two states. This would in fact be exactly what one would expect if the resource controlling oscillations is constantly produced and utilized, at slightly different rates or times in each cell.

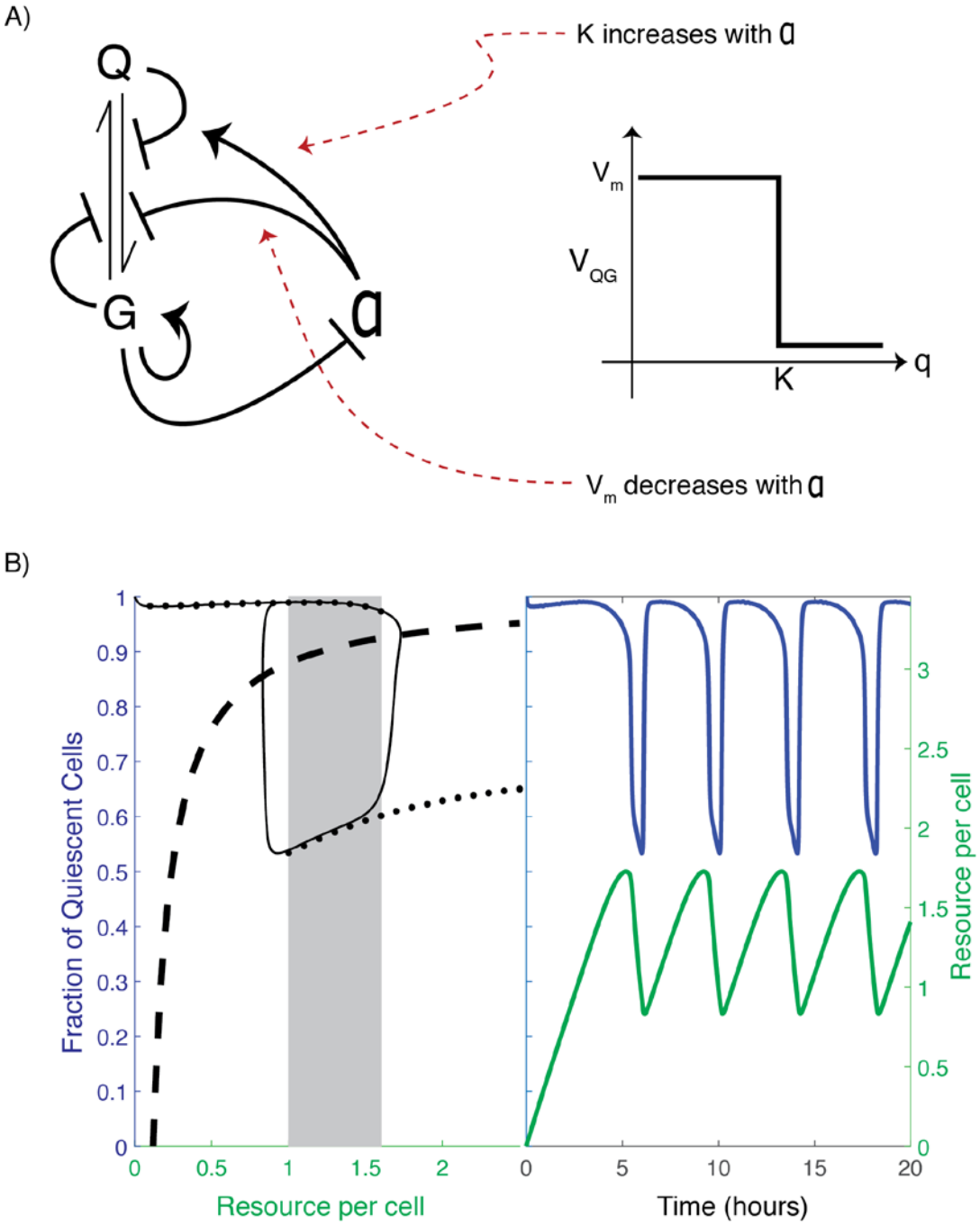

Figure 3: Fixing the pattern of the oscillation

A) Altering the communication loops between Q, G and a, to change the overall step-function. Here γ (growth rate) is constant, ν_{QG} is a decreasing step-function of q, and both the high and low levels of the step decrease with a

B) Resultant oscillations obtained (see Methods for the equations that produce this dynamics). Note that now the fast drop is followed by a slow drop, and then a fast rise, similar to the experimentally observed oscillations in Fig 1.

Predicting oscillatory outcomes based on resource availability

We have used scenario 3c to produce oscillations in Figures 2 and 3 above. We reiterate that mathematically scenarios 2 and 3 are the same, so scenario 2c can produce exactly the same oscillations. Further, we also find that scenario 1c (where the resource is not supplied externally, but produced/secreted by only the Q cells) is also capable of producing similar oscillations, based on some constrained choices for how the production rate of the resource (σ) depends on q and final a (see supplementary Fig S3). Thus, while scenarios 3c and 2c are identical, all three scenarios, 1c, 2c, 3c, with appropriate choices for how the switching rates, and production and consumption depend on the resource and fraction of quiescent cells, are sufficient to explain the YMC oscillations. Scenario 2c and 3c are largely indistinguishable, and both are biologically plausible. Given our experimental understanding of the YMC (and the need for a consumable resource, glucose, to control the oscillations), we think scenario 3c is most likely (and we will explore this further in a subsequent section).

Breakdown of the oscillations.

In Figs 2 and 3 above, we have chosen the particular "default" values of each of the model parameters such that the oscillation period became approximately 4 hours, to match the experimental observations in Fig 1. Of course, varying these parameter values changes the time period, and for large enough variation the oscillation may also disappear. Our model predicts how the oscillation shape and period will vary, and when oscillations will break down, in response to experimentally tunable parameters. For instance, Figure 4A shows how the oscillations change as the resource production rate, σ, is varied around its default value, for the same equations that produced the oscillations in Figs 2 and 3. When σ is decreased below the default value, the oscillation period initially increases without significant change in the shape of the oscillations. For low enough σ, the model first exhibits damped oscillations, and then as σ is lowered further, the model exhibits the absence of oscillations, with q settling into a high steady-state value (see also supplementary Fig S4 for more such plots) (Figure 4A). When σ is increased from its default value, we again find that the period initially decreases without much change in the shape. We are able to produce oscillations having a time period as low as ~2.5 hours (see Figure 4A(iii)). When σ is increased beyond this, the oscillation period starts increasing again, and the slow drop phase of the oscillation starts becoming pronounced (see supplementary Fig S4). Eventually, the oscillations disappear, with q settling into a (relatively) low steady-state value. These predictions largely mirror known experimental observations, where decreasing or increasing feed rate (at these scales) control oscillations similarly.

The resource production rate σ is a parameter that can be tuned relatively easily in a chemostat by controlling the amount of fresh glucose or ethanol being supplied per unit time. However, another parameter that may be tunable by genetic modifications is γ, the growth rate of cells when they are in the G state. Fig 4B shows how the oscillations vary as γ is varied. The results are qualitatively similar but inverse to what was observed with σ variation - an increase in γ results in decreasing period, damped oscillations and eventually no oscillations, while a

decrease first results in an increase of period, then a distorted shape and decreasing period (see supplementary Fig S5 for more such plots).

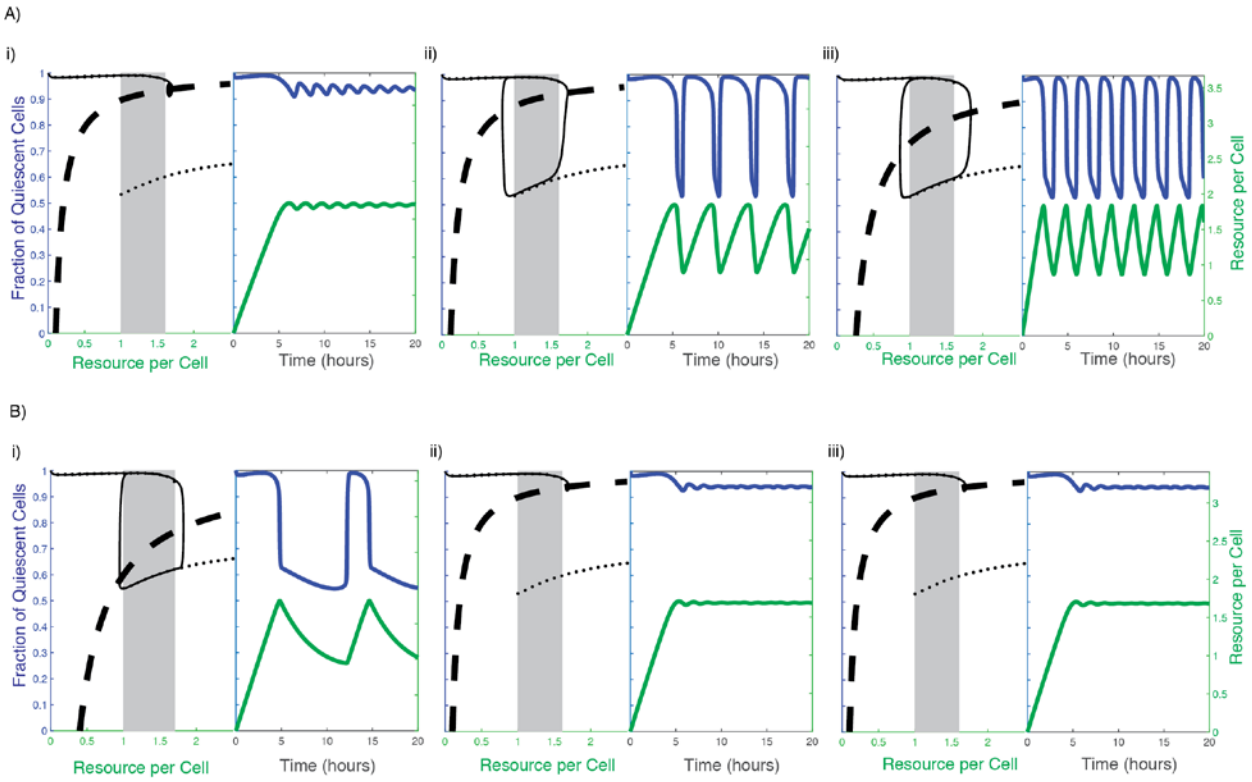

Figure 4: Breakdown of oscillations.

A) Varying the rate of production of resource σ. (i) $\sigma = 0.346\ \mathrm{hr}^{-1}$, (ii) $\sigma = 0.400\ \mathrm{hr}^{-1}$ (default parameters, same as Fig 3), (iii) $\sigma = 0.866\ \mathrm{hr}^{-1}$.

B) Varying the growth rate of cells γ. (i) $\gamma = 0.500\ \mathrm{hr}^{-1}$, (ii) $\gamma = 1.665\ \mathrm{hr}^{-1}$ (default parameters, same as Fig 3), (iii) $\gamma = 2.000\ \mathrm{hr}^{-1}$.

Acetyl-CoA and NADPH satisfy the requirements of the consumable resource that controls oscillations between Q and G states

Based on our model, the metabolic resource oscillates with a unique pattern, and this drives the oscillation between the Q and G states. Here, the resource builds up within the cell, and is highest at the point of commitment to the switch to the G state (Figure 5A). It is then rapidly consumed to fall below a certain threshold, resetting the oscillation, after which the cycle of building up for consumption resumes. When superimposed to the actual YMC phases (and the Q to G switch), this build-up of the resource would necessitate highest amounts of this resource at the beginning of the phase where cells commit to entering high oxygen consumption (Figure 5A). A second implication of this model is that once this resource hits the threshold level, the growth phase is committed, and cells will grow unimpeded as they consume this resource. This means that once committed to the growth switch, the growth/division rate is constant and now no longer variable based on other factors. Therefore, in order for any

metabolite to be the resource that controls the oscillation between the two states, this molecule must fully satisfy the above criteria. Furthermore, for completing this switch to the G state, the metabolite must be able to drive all the downstream biological events for growth. So do any central metabolites satisfy these requirements, and could therefore be the internal resource that controls these Q-G oscillations?

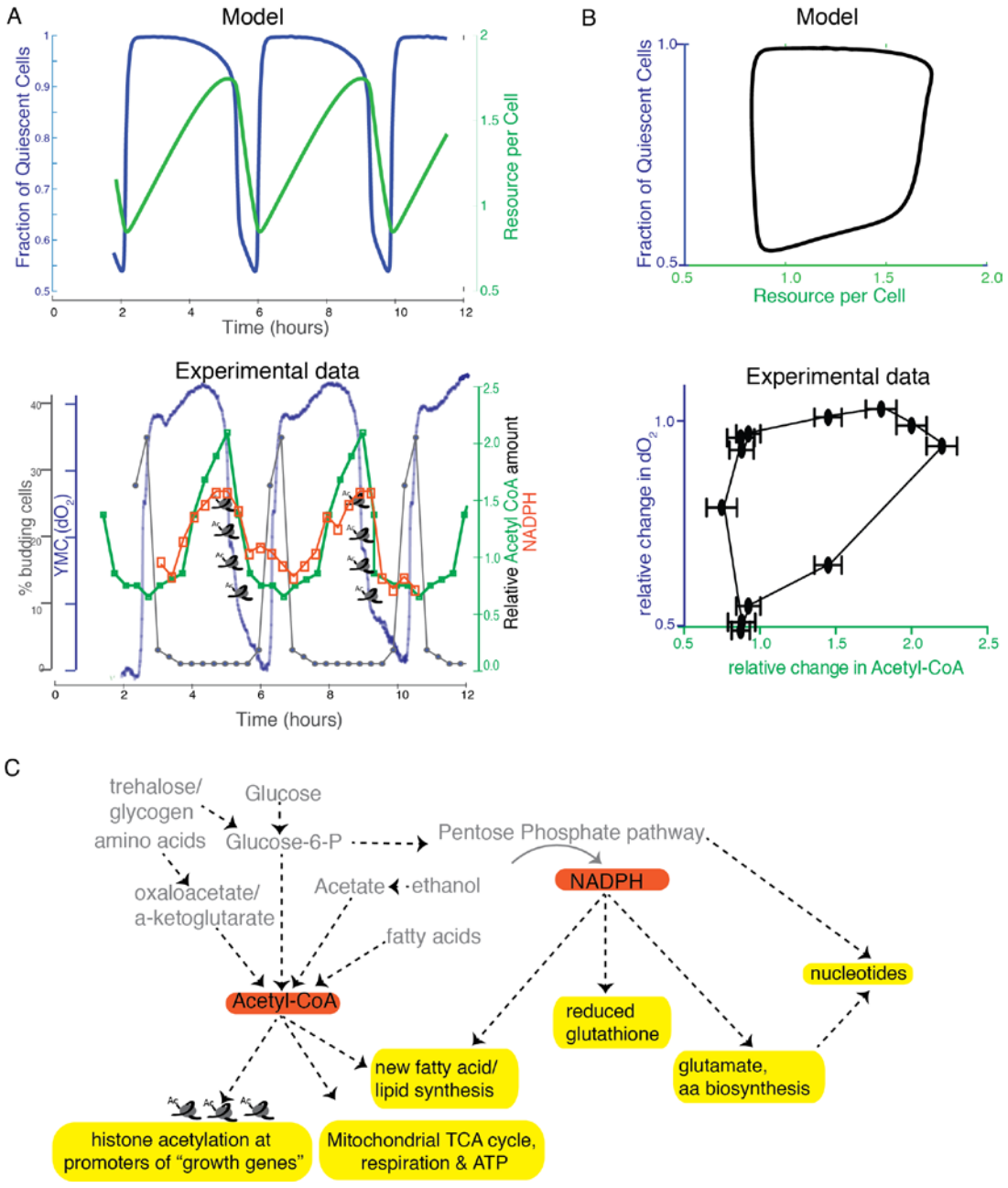

Figure 5: Acetyl-CoA satisfies the requirements for the metabolic resource controlling the Q and G oscillations.

A) Predicted pattern of oscillation of the resource, during the Q and G oscillations, based on the model (top panel, same as Fig 3), and experimentally observed oscillations of acetyl-CoA and NADPH during the dO_2 oscillations (bottom panel).

B) Predicted phase portrait of the the fraction of quiescent cells vs the resource per cell based on the model (top panel), and experimentally observed oscillations in dO_2 and acetyl-CoA.
C) Acetyl-CoA as a central regulator of a switch to the growth (G) state. The schematic illustrates a cascade of biological processes leading to growth that acetyl-CoA amounts regulate (coupled with coincident, required NADPH utilization).

Comprehensive datasets of oscillating metabolites in the YMC exist (46, 50). From these studies, the oscillations of two metabolites, acetyl-CoA and NADPH, fully fit the criteria demanded by our model. The acetyl-CoA and NADPH oscillations as a function of the metabolic cycle, and transitions between the Q and G state are shown in Figure 5A and 5B. The oscillations of acetyl-CoA during the YMC almost perfectly superimposes with the oscillation pattern of the theoretical metabolic resource predicted by the model (Figure 5A). Strikingly, the phase diagram of the fraction of quiescent cells vs the amount of resource in the cell almost perfectly reflects experimental data for the dO_2 oscillations plotted against acetyl-CoA amounts (Figure 5B). This is despite the fact that the experimental data for acetyl-CoA is of low resolution, with only a few sampling/time points covered, and also only reflects overall (bulk population) measurements of acetyl-CoA, suggesting that the actual phase diagram might be even more similar.

Multiple lines of experimental data also suggest that these two metabolites are key in controlling exit from quiescence and entry into growth (14, 34, 43, 45–47, 51). Based on our knowledge of the metabolic prerequisites for entering growth, and known functional endpoints or outcomes of these two molecules (Figure 5C), we can make a parsimony based argument suggesting that oscillations in these two metabolites are sufficient to control oscillations between the Q and G state. Particularly, several lines of study suggest that the entry into growth (from quiescence) depends on carbon source utilization (9, 15, 43, 44). Studies from the yeast metabolic cycle show that the oscillations depend upon carbon sources (primarily glucose) (33, 35), and oscillations can be reset (to enter the growth program) by adding acetate, acetaldehyde, etc. (33, 43). Notably, all these carbon sources end up being converted to acetyl-CoA, and then utilized (Figure 5C). Second, a growth program will require not just sufficient energy (ATP) to sustain the anabolic processes within it, but also activate a program boosting anabolic processes that lead to cell division, including making enough lipid moieties required for cell membranes and other constituents of a new cell. Acetyl-CoA satisfies all these requirements (Figure 5C): it directly enters the TCA cycle to generate ATP (52); it can be utilized for the biosynthesis of numerous cellular metabolites, including fatty acids, sterols, and amino acids (Lehninger); and directly regulates cell growth and ribosome biogenesis by the acetylation of histones at “growth promoting genes”, especially histones at ribosome subunit, tRNA and ribi genes, and activates their transcription by the SAGA complex (43). The genes that breakdown storage carbohydrates (such as glycogen and trehalose) that produce acetyl-CoA all peak *before* the maximal acetyl-CoA concentration (33, 48). Finally, the exit from quiescence requires the liquidation of these storage carbohydrates (15, 44, 45), and conversion to acetyl-CoA (and the subsequent gene expression program) (45). Perturbations in the ability to sense and utilize acetyl-CoA (particularly for the gene expression program) completely abolish oscillations (43). Physiologically, this anabolic commitment also absolutely requires the

process of reduction for anabolic biosynthesis, and this reductive capacity is supplied by NADPH (52) (Figure 5C). NADPH is primarily synthesized from the pentose phosphate pathway, which branches from this same central carbon network (Figure 5C), and this NADPH will fuel the required reductive biosynthesis to make molecules required for anabolism (Figure 5C). Finally, genes encoding proteins that increase the synthesis of NADPH are similarly coincident with those that lead to the generation of acetyl-CoA, and disrupting NADPH production slightly results in a collapse of oscillations (33, 46). Without a necessary coupling of the two molecules, the overall process of entry to growth cannot be completed. There is substantial data, particularly from the studies of various cancers, to show the close coupling of acetyl-CoA and NADPH for growth (53), as well as direct evidence of acetyl-CoA promoting NADPH synthesis (54, 55). Summarizing, based on the pattern of oscillation of the resource predicted by our model, acetyl-CoA and NADPH (based on production and utilization) satisfy requirements to be the molecules that control the Q-G state oscillations.

Discussion

In this study, we present a simple bistability model to explain how the amounts of an internal metabolic resource can determine oscillations between a quiescent and growth state. For this, we relied on extensive data coming from the YMC, and represented the oscillations in dissolved oxygen (seen during YMCs) as a reflection of growth and quiescent states (Figure 1). Our model incorporates factors dependent on growth rate and amounts of the resource, as well as switching rates (between the G and Q states) (Figures 2-4). Importantly, the model emphasizes a necessary communication between the cells in the quiescent state and the growth state, both of which interact with the metabolic resource during such transitions (Figures 2 and 3). Quiescent cells “push” cells in the growth state into quiescence, and “pull” other quiescent cells to remain quiescent, with the feedback requirements imposed by the resource being distinct and opposite for the Q and G states. Given this communication requirement between the Q and G states, our model suggests that such oscillations will eventually breakdown when the cell numbers are small and cells are no longer in contact with each other (something that has been experimentally observed (42)). This model also provides insight into understanding the “growth/division” rate of cells once committed to growth. While healthy debates continue on the rate of growth in a cell and stages of the cell cycle (36, 56–59) our model supports a fixed “growth rate” once the metabolic resource has crossed its threshold concentration, and triggered a committed growth program, after which the growth and division process is no longer dependent on available nutrients. This is consistent with studies of the CDC, which is built around committed, “no return” steps that proceed at constant, predictable rates once committed to. Finally, using a parsimony based argument, we suggest that acetyl-CoA (along with NADPH) satisfies all requirements for the resource that drive these oscillations between the Q and G states (Figure 5). We reiterate that our model only provides a paradigm to explain how the oscillations in an internal metabolic resource is *sufficient* to control oscillations between quiescent and growth states. This allows for (but doesn’t include) other necessary elements in cells (e.g., unique gene transcription programs), that may also be required to build a more detailed model for Q-G oscillations.

The kind of oscillator we have built falls under the class of “relaxation oscillators”, which have been used to model a very wide variety of phenomena, ranging from electronic oscillations to oscillating chemical reactions (60, 61). These are a subset of several possible types of oscillators that arise in biological systems, and are especially relevant for the CDC (19, 28, 62, 63). Relaxation oscillators typically involve the cyclic slow build-up of some quantity, like charge in a capacitor, until it reaches a threshold level which then triggers a “discharge” event, resulting in a rapid drop of the quantity. Thus, relaxation oscillators are often characterised by processes happening on two very different timescales, with the time period mainly determined by the slow process (17, 19, 28, 62, 63). This is why, in contrast to linear, harmonic oscillators, they can produce non-smooth oscillations like a square or sawtooth waveform. The YMC oscillations show a clear signature of multiple timescales - in Fig 1 it is evident that the exit from quiescence (fast drop in dO2), as well as the re-entry into quiescence (fast rise in dO2), happen at much faster timescales than the other phases of the oscillation. In our relaxation oscillator model of the YMC, these differing timescales arise from the fact that the switching rates are an order of magnitude larger than the rates of production and consumption of the resource, and even the growth rate of the cells. The latter processes are therefore what determine the time period of the YMC. Within the class of relaxation oscillators, our models fall into a sub-class that depends on an underlying bistability, which is `frustrated’ (49). The bistability, and the resultant hysteresis, are what determine the threshold points at which the behaviour of the system rapidly switches between accumulating or consuming the metabolic resource. Interestingly, our model necessitates a strong hysteresis element within these Q and G state cells. The phenomenon of hysteresis has been extremely well studied (and established) particularly during many phases of the classical CDC, or proliferation cycle ((16, 19, 24, 63–68) and many more). In contrast, a hysteresis phenomenon has not been extensively explored when cells transition between a growth state and an effective quiescence state. Yet, in such conditions where the transition between the two states is substantially determined by a metabolic oscillator, as seen in the YMC and several other studies from simple models like yeast, the hysteresis phenomenon is both clearly and apparently revealed by our model. Given this, experimental studies can be designed to dissect the nature of this hysteresis phenomenon.

Finally: Given the existing frameworks to describe Q-G state oscillations, our model is necessarily coarse grained, and is intended only to build a more rigorous conceptual framework within which to investigate the process of cells switching between quiescence and growth states. For instance, it is straightforward to extend our models, by adding space and diffusion processes, to account for scenarios where nutrients are not well mixed and equally accessible, and where there is a high degree of spatial rigidity within cell populations. Currently, existing experimental approaches to study such metabolically-driven Q-G oscillations are very limited. Crude readouts, such as oxygen consumption, have very limited resolution even to show the Q and G states, as the bistability begins to break down. Gene expression analysis (even when done in single cells) is a late, end-point readout which cannot explain this bistability but instead occurs after a switch. The key to experimentally studying such bistability, therefore, will be the development of *in vivo* intracellular metabolic sensors with excellent dynamic range and sensitivity, for metabolites like acetyl-CoA or NADPH. This will allow the development of more

precise models to predict commitment steps, and identify differences within the population of cells, that will help understand reversibility (between states), hysteresis and other apparent phenomena.

Methods

Experimental methods and data sets:

Chemostat culture and cell division datasets: All dO_2 data were obtained from YMCs set up similar to already published data (33, 46, 48). In these studies, yeast cells were grown in chemostat cultures using semi-defined medium, and yeast metabolic cycles were set up as described earlier (33, 69). Data for cell division across three metabolic cycles was obtained from earlier studies (33, 42). YMC gene expression and metabolite datasets: Gene expression datasets were obtained from (33, 48), and metabolite oscillation datasets were obtained from (43, 46, 47, 50), including acetyl-CoA oscillation datasets.

Two-state model with switching between the states and growth in only one of the states

Let $Q(t)$ be the number of cells in the quiescent state at time t, and $G(t)$ the number of cells in the growing/dividing state. A model for a well-mixed chemostat that includes switching between these states, as well as dilution from the chemostat outflux, can be described by the following equations:

$$\frac{dQ}{dt} = \nu_{GQ}G - \nu_{QG}Q - \phi(t)Q, \qquad (3)$$

$$\frac{dG}{dt} = \gamma G - \nu_{GQ}G + \nu_{QG}Q - \phi(t)G, \qquad (4)$$

where each ν represents a switching rate, ϕ is the chemostat outflux rate (which could vary with time), and γ is the growth rate of cells in the growing/dividing state. Let's further assume the chemostat is working in a mode that maintains the total population (or optical density) of cells at some constant level, i.e., the outflux from the chemostat balances the growth of cells at all times, which means $\phi(t) = \gamma G/(G+Q)$. In this case, the population dynamics can be described by a single equation:

$$\frac{dq}{dt} = \nu_{GQ}(1-q) - \nu_{QG}q - \gamma q(1-q), \qquad (5)$$

where $q \equiv Q/(G+Q)$ is the *fraction* of cells in the quiescent state. This is the same as equation 1 in the Results section.

Next, we assume that the cells contain some `resource' that they require for growth. Let $a(t)$ denote the concentration per cell of this resource at time *t*, and let σ denote the (constant) rate at which additional amounts of this resource enter each cell from the surroundings (where the resource is replenished due to the influx of fresh medium into the chemostat). a is depleted both by dilution due to the outflux (at a rate $\gamma(1-q)$ as explained above), as well as by consumption

by growing cells (this rate is also proportional to $\gamma(1-q)$, which is the net rate of production of new cells). The dynamics of this resource can thus be described by the equation:

$$\frac{da}{dt} = \sigma - \mu\gamma(1-q)a - \gamma(1-q)a, \qquad (6)$$

where μ is a proportionality constant that sets just how much resource is consumed by a growing cell, compared to the amount that is depleted by dilution. This is the same as equation 2 in the Results section.

In writing equations 5 and 6, we have assumed that all cells have the same amount of this internal resource a. A less restrictive assumption that still gives the same equation is to assume that a represents the average concentration of the resource across the population of cells. Further, the same equations also model the case where the resource is not an intracellular one, but an extracellular one - σ then is just reinterpreted as the rate at which the resource is added to the extracellular medium either by an external feed or by secretion of the resource by the cells themselves (e.g., by making σ dependent on q).

To produce Fig 2C, we make the following choices (within scenario 3c):
$\gamma = 0.32\times a\ hr^{-1}$, $\sigma = 0.32\ hr^{-1}$, $\mu = 1$,$v_{QG} = 0.32\ hr^{-1}$, $v_{GQ} = [1 + 1.8\times\theta(q-0.9)]\times 32\ hr^{-1}$, where $\theta(x)$ is the step-function, which is zero for $x < 0$ and unity for $x > 0$. We approximate the step function using a Hill equation with a very high Hill coefficient: $\theta(x-K) = \frac{\left(\frac{x}{K}\right)^{20}}{1+\left(\frac{x}{K}\right)^{20}}$.

To produce Fig 3B, 5A and 5B, we make the following choices (within scenario 3c):
$\gamma = 1.665\ hr^{-1}$, $\sigma = 0.3996\ hr^{-1}$, $\mu = 1$,$v_{QG} = v[1 - 0.99\times\theta(q-K)]$, $K = a^2/(0.75^2 + a^2)$, $v = (0.165 - 0.125K)\ hr^{-1}$, $v_{GQ} = 16.65\ hr^{-1}$, where $\theta(x)$ is the step-function, which is zero for $x < 0$ and unity for $x > 0$ (approximated as above). Figure 4 panels are made using the same equations, but varying the values of σ and γ.

Acknowledgements

SK is supported by funds from the Simons Foundation, and institutional support from NCBS-TIFR. SL is supported by a Wellcome Trust-DBT IA intermediate fellowship (IA/I/14/2/501523), and institutional support from inStem and the Department of Biotechnology.

References

1. Gray, J. V, Petsko, G. a, Johnston, G. C., Ringe, D., Singer, R. a, and Werner-washburne, M. (2004) Sleeping Beauty : Quiescence in Saccharomyces cerevisiae " Sleeping Beauty ": Quiescence in Saccharomyces cerevisiae †. *Microbiol. Mol. Biol. Rev.* **68**, 187–206
2. Lewis, D., and Gattie, D. (1991) The Ecology of Quiescent Microbes. *U.S. Environ. Prot. Agency, Washington, D.C.*
3. Cooper, S. (1998) On the proposal of a G0 phase and the restriction point. *FASEB J.* **12**, 367–373
4. Cooper, S. (2003) Reappraisal of serum starvation, the restriction point, G0, and G1 phase arrest points . *FASEB J.* **17**, 333–340
5. Coller, H. A., Sang, L., and Roberts, J. M. (2006) A New Description of Cellular Quiescence. *PLoS Biol.* **4**, e83
6. Klosinska, M. M., Crutchfield, C. A., Bradley, P. H., Rabinowitz, J. D., and Broach, J. R. (2011) Yeast cells can access distinct quiescent states. *Genes Dev.* **25**, 336–49
7. Dhawan, J., and Laxman, S. (2015) Decoding the stem cell quiescence cycle - lessons from yeast for regenerative biology. *J. Cell Sci.* **128**, 4467–4474
8. De Virgilio, C. (2012) The essence of yeast quiescence. *FEMS Microbiol. Rev.* **36**, 306–339
9. Daignan-Fornier, B., and Sagot, I. (2011) Proliferation/Quiescence: When to start? Where to stop? What to stock? *Cell Div.* **6**, 20
10. Kalucka, J., Missiaen, R., Georgiadou, M., Schoors, S., Lange, C., Bock, K. De, Dewerchin, M., Carmeliet, P., Kalucka, J., Missiaen, R., Georgiadou, M., and Schoors, S. (2015) Metabolic control of the cell cycle. 10.1080/15384101.2015.1090068
11. Kaplon, J., Dam, L. Van, Peeper, D., Kaplon, J., Dam, L. Van, and Peeper, D. (2015) Two-way communication between the metabolic and cell cycle machineries : the molecular basis. *Cell Cycle*. **14**, 2022–32
12. Futcher, B. (2006) Metabolic cycle , cell cycle , and the finishing kick to Start. 10.1186/gb-2006-7-4-107
13. Lee, I. H., and Finkel, T. (2013) Metabolic regulation of the cell cycle. *Curr. Opin. Cell Biol.* **25**, 724–729
14. Cai, L., and Tu, B. P. (2012) Driving the Cell Cycle Through Metabolism. *Annu. Rev. Cell Dev. Biol.* **28**, 59–87
15. Laporte, D., Lebaudy, A., Sahin, A., Pinson, B., Ceschin, J., Daignan-Fornier, B., and Sagot, I. (2011) Metabolic status rather than cell cycle signals control quiescence entry and exit. *J. Cell Biol.* **192**, 949–957
16. TYSON, J. J., and NOVAK, B. (2001) Regulation of the Eukaryotic Cell Cycle: Molecular Antagonism, Hysteresis, and Irreversible Transitions. *J. Theor. Biol.* **210**, 249–263
17. Tyson, J. J., Chen, K. C., and Novak, B. (2003) Sniffers, buzzers, toggles and blinkers: Dynamics of regulatory and signaling pathways in the cell. *Curr. Opin. Cell Biol.* **15**, 221–231
18. Tyson, J. J., and Novák, B. (2015) Models in biology: lessons from modeling regulation of the eukaryotic cell cycle. *BMC Biol.* **13**, 46
19. Ferrell, J. E., Pomerening, J., Kim, S. Y., Trunnell, N. B., Xiong, W., Huang, C.-Y. F., and Machleder, E. M. (2009) Simple, realistic models of complex biological processes: Positive feedback and bistability in a cell fate switch and a cell cycle oscillator. *FEBS Lett.* **583**, 3999–4005
20. Norel, R., and Agur, Z. (1991) A model for the adjustment of the mitotic clock by cyclin and MPF levels. *Science (80-.).* **251**, 1076–8
21. Goldbeter, A. (1991) A minimal cascade model for the mitotic oscillator involving cyclin

and cdc2 kinase. *Proc. Natl. Acad. Sci.* **88**, 9107–9111
22. TYSON, J. J. (1991) Modeling the cell division cycle: cdc2 and cyclin interactions. *Proc. Natl. Acad. Sci.* **88**, 7328–7332
23. Novak, B., and Tyson, J. J. (1993) Numerical analysis of a comprehensive model of M-phase control in Xenopus oocyte extracts and intact embryos. *J. Cell Sci.* **106**, 1153–1168
24. Wei, S., Moore, J., Chen, K., Lassaletta, A. D., Yi, C.-S., Tyson, J. J., and Sible, J. C. (2003) Hysteresis drives cell-cycle transitions in Xenopus laevis egg extracts. *Proc. Natl. Acad. Sci.* **100**, 975–980
25. Pomerening, J., Sontag, E., and Ferrell, J. E. (2003) Building a cell cycle oscillator: hysteresis and bistability in the activation of Cdc2. *Nat. Cell Biol.* **5**, 346–51
26. Cross, F., Archambault, V., Miller, M., and Klovstad, M. (2002) Testing a mathematical model of the yeast cell cycle. *Mol. Biol. Cell*. **13**, 52–70
27. Mirchenko, L., and Uhlmann, F. (2010) Sli15(INCENP) dephosphorylation prevents mitotic checkpoint reengagement due to loss of tension at anaphase onset. *Curr. Biol.* **20**, 1396–401
28. Novák, B., and Tyson, J. J. (2008) Design principles of biochemical oscillators. *Nat. Rev. Mol. Cell Biol.* **9**, 981–991
29. Hartwell, L. H. (1974) Saccharomyces cerevisiae cell cycle. *Bacteriol. Rev.* **38**, 164–198
30. Daignan-Fornier B and Sagot I (2011) Proliferation / quiescence : the controversial " aller-retour ." *Cell Div.* **6**, 2–5
31. Jules, M., François, J., and Parrou, J. L. (2005) Autonomous oscillations in Saccharomyces cerevisiae during batch cultures on trehalose. *FEBS J.* **272**, 1490–1500
32. Keulers, M., Suzuki, T., Satroutdinov, A., and Kuriyama, H. (1996) Autonomous metabolic oscillation in continuous culture of Saccharomyces cerevisiae grown on ethanol. *FEMS Microbiol. Lett.* **142**, 253–8
33. Tu, B. P., Kudlicki, A., Rowicka, M., and McKnight, S. L. (2005) Logic of the yeast metabolic cycle: temporal compartmentalization of cellular processes. *Science*. **310**, 1152–1158
34. Mellor, J. (2016) The molecular basis of metabolic cycles and their relationship to circadian rhythms. *Nat. Struct. Mol. Biol.* **23**, 1035–1044
35. Klevecz, R. R., Bolen, J., Forrest, G., and Murray, D. B. (2004) A genomewide oscillation in transcription gates DNA replication and cell cycle. *Proc. Natl. Acad. Sci.* **101**, 1200–1205
36. Brauer, M. J., Huttenhower, C., Airoldi, E. M., Rosenstein, R., Matese, J. C., Gresham, D., Boer, V. M., Troyanskaya, O. G., and Botstein, D. (2008) Coordination of Growth Rate, Cell Cycle, Stress Response, and Metabolic Activity in Yeast. *Mol. Biol. Cell*. **19**, 352–267
37. Rowicka, M., Kudlicki, A., Tu, B. P., and Otwinowski, Z. (2007) High-resolution timing of cell cycle-regulated gene expression. *Proc. Natl. Acad. Sci. U. S. A.* **104**, 16892–7
38. Slavov, N., and Botstein, D. (2013) Decoupling nutrient signaling from growth rate causes aerobic glycolysis and deregulation of cell size and gene expression. *Mol. Biol. Cell*. **24**, 157–168
39. Slavov, N., and Botstein, D. (2011) Coupling among growth rate response, metabolic cycle, and cell division cycle in yeast. *Mol. Biol. Cell*. **22**, 1997–2009
40. Küenzi, M. T., and Fiechter, A. (1969) Changes in carbohydrate composition and trehalase-activity during the budding cycle of Saccharomyces cerevisiae. *Arch. Mikrobiol.* **64**, 396–407
41. Robertson, J. B., Stowers, C. C., Boczko, E., and Johnson, C. H. (2008) Real-time luminescence monitoring of cell-cycle and respiratory oscillations in yeast. *Proc. Natl. Acad. Sci. U. S. A.* **105**, 17988–93

42. Laxman, S., Sutter, B. M., and Tu, B. P. (2010) Behavior of a metabolic cycling population at the single cell level as visualized by fluorescent gene expression reporters. *PLoS One*. **5**, e12595
43. Cai, L., Sutter, B. M., Li, B., and Tu, B. P. (2011) Acetyl-CoA induces cell growth and proliferation by promoting the acetylation of histones at growth genes. *Mol. Cell*. **42**, 426–37
44. Shi, L., Sutter, B. M., Ye, X., and Tu, B. P. (2010) Trehalose is a key determinant of the quiescent metabolic state that fuels cell cycle progression upon return to growth. *Mol. Biol. Cell*. **21**, 1982–90
45. Shi, L., and Tu, B. P. (2013) Acetyl-CoA induces transcription of the key G1 cyclin CLN3 to promote entry into the cell division cycle in Saccharomyces cerevisiae. *Proc. Natl. Acad. Sci.* **110**, 7318–7323
46. Tu, B. P., Mohler, R. E., Liu, J. C., Dombek, K. M., Young, E. T., Synovec, R. E., and McKnight, S. L. (2007) Cyclic changes in metabolic state during the life of a yeast cell. *Proc. Natl. Acad. Sci. U. S. A.* **104**, 16886–16891
47. Machné, R., and Murray, D. B. (2012) The yin and yang of yeast transcription: elements of a global feedback system between metabolism and chromatin. *PLoS One*. **7**, e37906
48. Kudlicki, A., Rowicka, M., and Otwinowski, Z. (2007) SCEPTRANS: an online tool for analyzing periodic transcription in yeast . *Bioinformatics*. **23**, 1559–1561
49. Krishna, S., Semsey, S., and Jensen, M. (2009) Frustrated bistability as a means to engineer oscillations in biological systems. *Phys. Biol.* **6**, 36009
50. Mohler, R., Tu, B. P., Dombek, K. M., Hoggard, J., Young, E., and Synovec, R. E. (2008) Identification and evaluation of cycling yeast metabolites in two-dimensional comprehensive gas chromatography-time-of-flight-mass spectrometry data. *J. Chromatogr. A*. **1186**, 401–11
51. Shi, L., and Tu, B. P. (2014) Protein acetylation as a means to regulate protein function in tune with metabolic state. *Biochem. Soc. Trans.* **42**, 1037–1042
52. Nelson, D. L., and Cox, M. M. (2013) *Lehninger Principles of Biochemistry.*, Seven, Macmillan
53. Heiden, M. G. Vander, Cantley, L. C., and Thompson, C. B. (2009) Understanding the Warburg Effect: The Metabolic Requirements of Cell Proliferation. *Science (80-.).* **324**, 1029–1033
54. Shan, C., Elf, S., Ji, Q., Kang, H. B., Zhou, L., Hitosugi, T., Jin, L., Lin, R., Zhang, L., Seo, J. H., Xie, J., Tucker, M., Gu, T. L., Sudderth, J., Jiang, L., DeBerardinis, R. J., Wu, S., Li, Y., Mao, H., Chen, P. R., Wang, D., Chen, G. Z., Lonial, S., Arellano, M. L., Khoury, H. J., Khuri, F. R., Lee, B. H., Brat, D. J., Ye, K., Boggon, T. J., He, C., Kang, S., Fan, J., and Chen, J. (2014) Lysine acetylation activates 6-phosphogluconate dehydrogenase to promote tumor growth. *Mol. Cell*. **55**, 552–565
55. Patra, K. C., and Hay, N. (2014) The pentose phosphate pathway and cancer. *Trends Biochem. Sci.* **39**, 347–354
56. Conlon, I., and Raff, M. (2003) Differences in the way a mammalian cell and yeast cells coordinate cell growth and cell-cycle progression. *J. Biol.*
57. Jorgensen, P., and Tyers, M. (2004) How Cells Coordinate Growth and Division. *Curr. Biol.* **14**, R1014–R1027
58. Goranov, A. I., Cook, M., Ricicova, M., Ben-Ari, G., Gonzalez, C., Hasen, C., Tyers, M., and Amon, A. (2009) The rate of cell growth is governed by cell cycle stage. *Genes Dev.* **23**, 1420–1422
59. Johnston, G. C., Pringle, J. R., and Hartwell, L. H. (1977) Coordination of growth with cell division in the yeast Saccharomyces cerevisiae. *Exp. Cell Res.* **105**, 79–98
60. Balthasar, van der P. (1926) “On Relaxation-Oscillations”. *London, Edinburgh, Dublin Philos. Mag.* **2**, 978–992

61. Strogatz, S. (1994) *Nonlinear Dynamics and Chaos.*, Addison-Wesley, Reading, MA
62. Tsai, T., Choi, Y., Ma, W., Pomerening, J., Tang, C., and Ferrell, J. E. (2008) Robust, tunable biological oscillations from interlinked positive and negative feedback loops. *Science (80-.).* **321**, 126–9
63. Ferrell, J. E. (2011) Simple Rules for Complex Processes: New Lessons from the Budding Yeast Cell Cycle. *Mol. Cell*. **43**, 497–500
64. Solomon, M. J. (2003) Hysteresis meets the cell cycle. *Proc. Natl. Acad. Sci.* **100**, 771–772
65. Pomerantz, S. C., and McCloskey, J. A. (1990) Analysis of RNA Hydrolyzates by Liquid Chromatography-Mass Spectrometry. *Methods Enzymol.* **193**, 796–824
66. Han, Z., Yang, L., MacLellan, R. W., Weiss, J. N., and Qu, Z. (2005) Hysteresis and Cell Cycle Transitions: How Crucial Is It? *Biophys. J.* **88**, 1626–1634
67. Yao, G., Tan, C., West, M., Nevins, J. R., and You, L. (2011) Origin of bistability underlying mammalian cell cycle entry. *Mol. Syst. Biol.* **7**, 485
68. Angeli, D., Ferrell, J. E., and Sontag, E. (2004) Detection of multistability, bifurcations, and hysteresis in a large class of biological positive-feedback systems. *Proc. Natl. Acad. Sci.* **101**, 1822–1827
69. Tu, B. P. (2010) Ultradian metabolic cycles in yeast. *Methods Enzymol.* **470**, 857–66

Supplementary material for

A minimal "push-pull" bistability model explains metabolite dependent oscillations between quiescent and proliferative cell states.

Sandeep Krishna and Sunil Laxman

1 Absence of oscillations

For reference, the equations we use are:

$$\frac{dq}{dt} = \nu_{GQ}(1-q) - \nu_{QG}q - \gamma(1-q)q, \quad (1)$$

$$\frac{da}{dt} = \sigma - \gamma(1-q)a. \quad (2)$$

To produce Fig 2C in the main text, we then used: $\gamma = 0.32 \times a\ hr^{-1}, \sigma = 0.32\ hr^{-1}, \mu = 1, \nu_{QG} = 0.32\ hr^{-1}, \nu_{GQ} = [1 + 1.8 \times \theta(q - 0.9)] \times 32\ hr^{-1}$, where $\theta(x)$ is the step-function, approximated by a Hill equation with a high Hill coefficient of 20. To produce Fig 3B, 5A and 5B in the main text, we used: $\gamma = 1.665\ hr^{-1}, \sigma = 0.3996\ hr^{-1}, \mu = 1, \nu_{QG} = \nu[1 - 0.99 \times \theta(q - K)], K = a^2/(0.75^2 + a^2), \nu = (0.165 - 0.125K)\ hr^{-1}, \nu_{GQ} = 16.65\ hr^{-1}$.

1.1 No oscillations in the absence of switching

When both ν_{GQ} and ν_{QG} are zero, then equation 1 above becomes:

$$\frac{dq}{dt} = -\gamma(1-q)q. \quad (3)$$

As long as γ is always positive, irrespective of its dependence on a, this has only one stable steady-state solution: $q = 0$ (not surprising because the rate of change of q is always negative). And this is globally stable, i.e., every initial value of q (except $q = 1$) will flow to $q = 0$. The $q = 1$ state is an unstable steady state, i.e., any fluctuations away from it, however small, will result in the system moving to $q = 0$. Thus, there can be no oscillations in the absence of switching.

1.2 No oscillations with constant parameters

When all the parameters in equations 1 and 2 are constants, then no oscillations are possible because eq. 1 becomes independent of eq. 2, and therefore, being a one dimensional ordinary differential equation without explicit time-dependence, cannot show oscillations (an oscillation in q requires that $\frac{dq}{dt}$ take both positive and negative values for the same value of q, for at least some range of q, and this is not possible for a 1D ordinary differential equation).

1.3 No oscillations for random switching

A less restrictive assumption is that ν_{GQ} and ν_{QG} are constants (which includes zero - we've already examined the case where both are zero above), but γ may be a function of a and σ may be a function of q and/or a. In the scenarios we examine, γ may be an increasing function of a (all scenarios), while σ may be an increasing function of q (scenario 1). In this situation, the dependence of each variable on the other is 'monotonic' ($\frac{dq}{dt}$ is a decreasing function of a, while $\frac{da}{dt}$ is an increasing function of q). Equations with such monotonic dependencies have been studied mathematically in detail in refs. (Pigolotti, Krishna, Jensen (2007) Proc. Natl. Acad. Sci 104, 6533; Tiana, Krishna, Pigolotti, Jensen, Sneppen (2007) Phys. Biol. 4, R1), which show explicitly that when such a coupled set of equations has only *two* variables (here, q and a), then sustained oscillations are not possible. Intuitively, there is not enough time delay in such a small two-leg feedback loop to destabilise the overall negative feedback that pulls the variables into a single stable steady-state value.

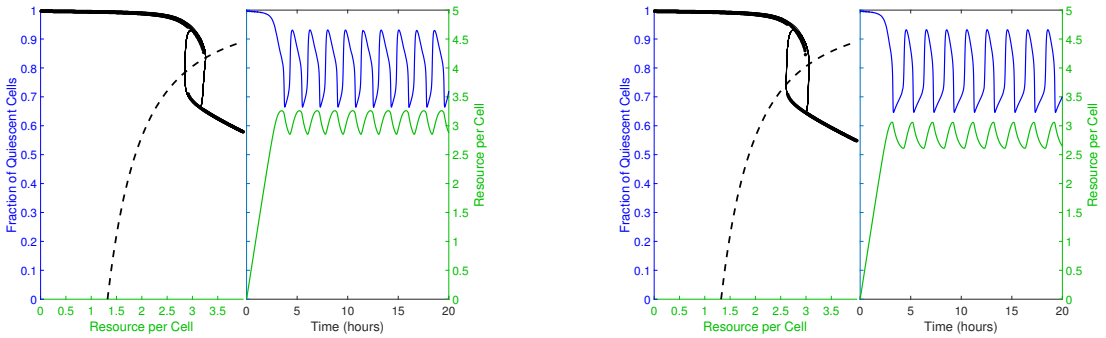

Figure S1: **Switching rate dependence on q that is sufficient to produce oscillations.** We have already shown, in Fig 2C in the main text, that choosing ν_{QG} to be constant and ν_{GQ} to be an increasing function of q is sufficient to produce oscillations: $\nu_{QG} = 0.32\ hr^{-1}, \nu_{GQ} = [1 + 1.8 \times \theta(q - 0.9)] \times 32\ hr^{-1}$, where $\theta(x)$ is the step-function, approximated by a Hill equation with a high Hill coefficient of 20. **(Left panel)** shows that choosing ν_{GQ} constant and ν_{QG} to be a decreasing function of q is also sufficient: $\nu_{QG} = [16 - 15.68 \times \theta(q - 0.75)]\ hr^{-1}, \nu_{GQ} = 96\ hr^{-1}$ (all other parameters same as in Fig 2C, except $\sigma = 1.13\ hr^{1}$). **(Right panel)** shows that choosing both as the above type of step function is also sufficient: $\nu_{QG} = [16 - 15.68 \times \theta(q - 0.75)]\ hr^{-1}, \nu_{GQ} = [1 + 1.8 \times \theta(q - 0.4)] \times 32\ hr^{-1}$ (all other parameters same as in Fig 2C, except $\sigma = 1.13\ hr^{1}$).

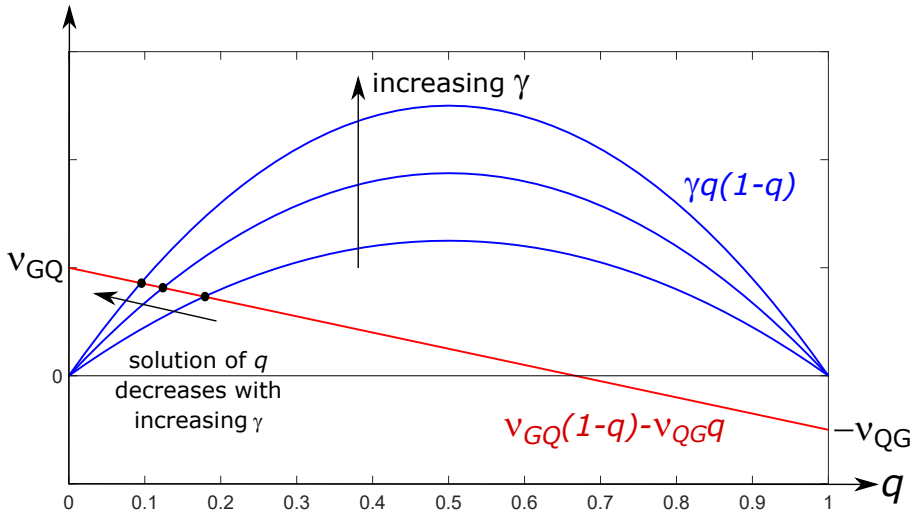

Figure S2: γ **proportional to** a **produces the wrong shape of oscillations.** In our scenario 3c equations used to generate Fig 2 in the main text, the lower branch of steady-states can be calculated as those that satisfy: $0 = \nu_{GQ}(1 - q) - \nu_{QG}q - \gamma(1 - q)q$, where $\nu_{GQ} = 32\ hr^{-1}$ (the lower value of the step function) and $\nu_{QG} = 0.32\ hr^{-1}$. The plot visualises, schematically, the solutions of this equation as the point where the curve $\gamma q(1 - q)$ intersects the straight line $\nu_{GQ}(1 - q) - \nu_{QG}q$. It is evident that if γ is an increasing function of a, then the solution, i.e., the steady-state of q, is a decreasing function of a. As explained in the main text, this is the opposite of what is required to get the correct shape of oscillations.

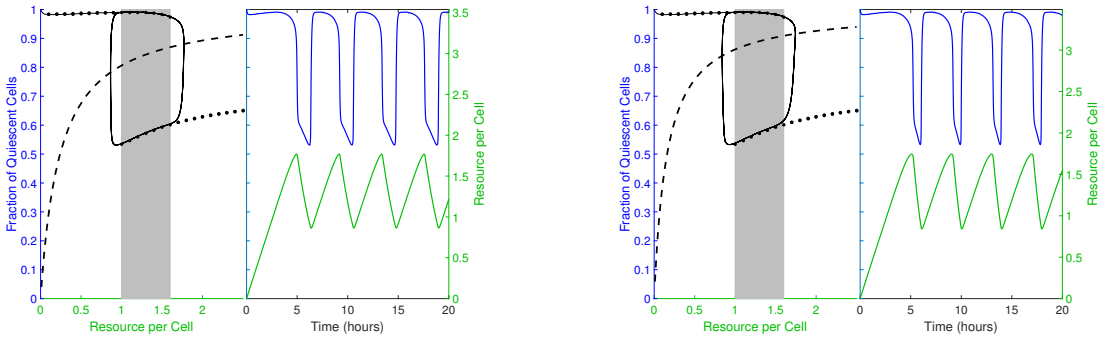

Figure S3: **Oscillations can also be produced in Scenario 1c.** Scenario 1c differs from Scenario 2c/3c in that σ is a function of q, not a constant, and potentially there is no consumption of the resource. Thus, the governing equation for q is no different from scenarios 2c/3c. Therefore, the bistability structure can be made mathematically identical by making exactly the same choices for ν_{GQ}, νQG and γ, as we made in Fig 3 in the main text. In order to get oscillations from this bistability structure, the requirement is that the second equation's 'null cline' pass between the lower and upper branches of steady states without intersection them (see ref. 50 in main text). The null cline is the line traced by the values of q and a that satisfy $\frac{da}{dt} = 0$ (dashed lines in Figs 2, 3 and 5 in the main text). For scenario 1, it is easy to find σ functions that are dependent on q in such a way as to do this, whether there is consumption of the resource or not. For example: **(left panel)** oscillations obtained in the extreme case of no consumption, when $\sigma = 0.3996 \times a\ hr^{-1}$, $\mu = 0$; **(right panel)** oscillations obtained when $\sigma = 0.3996 \times a\ hr^{-1}$, $\mu = 0.5$ (half of what was used in Fig 3 in the main text). In both plots, all other parameters are chosen as in Fig 3 in the main text.

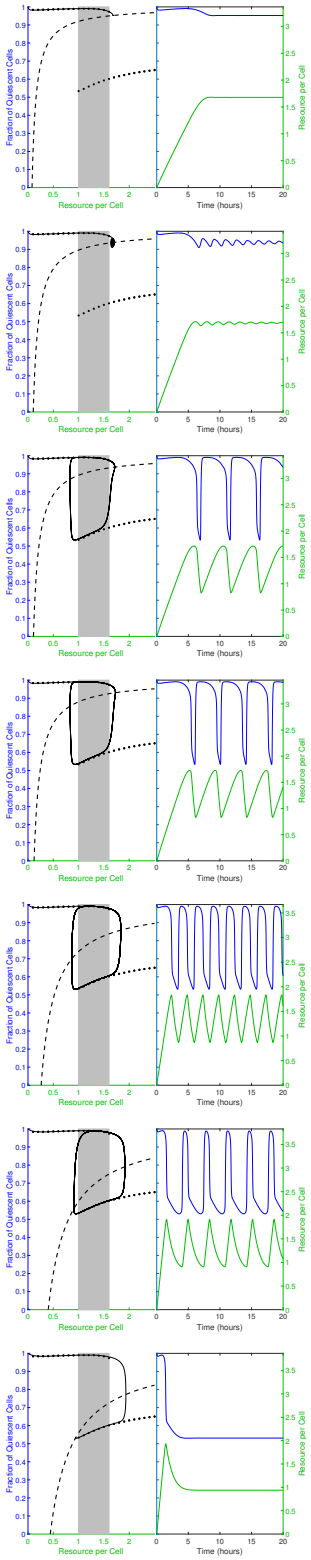

Figure S4: **Varying σ in equations that produced Fig 3,4 in the main text.** Top to bottom: $\sigma = 0.2664, 0.3463, 0.3596, 0.3996, 0.8658, 1.3320, 1.4652\ hr^{-1}$.

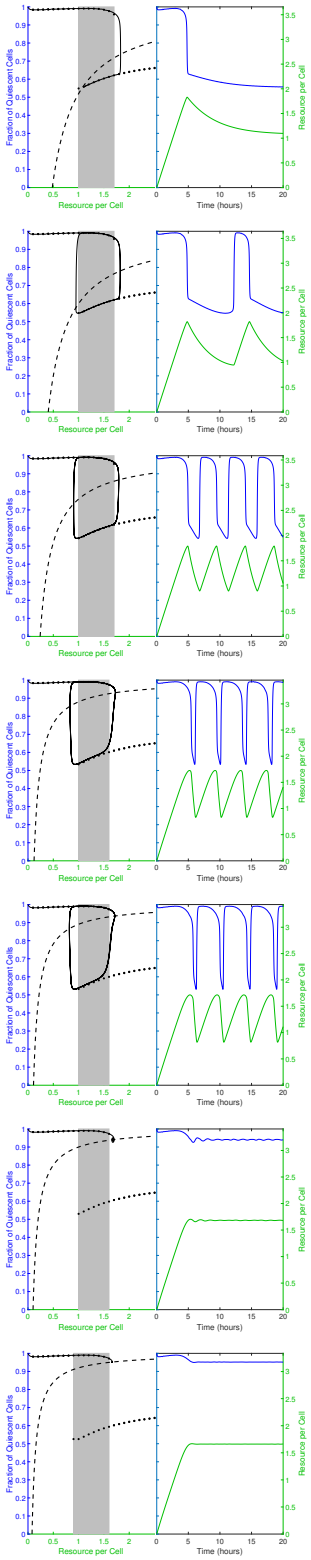

Figure S5: **Varying γ in equations that produced Fig 3,4 in the main text.** Top to bottom: $\gamma = 0.4163, 0.4995, 0.8325, 1.6650, 1.8315, 1.9980, 2.4975\ hr^{-1}$.